Université Libre de Bruxelles
Faculté des Sciences
Département d'Informatique

Master en sciences informatiques

MEMO–F508 Masters thesis

Cartographie 3D du système lymphatique par imagerie IR

Nascimento Gustavo
Promoteur: Prof. Olivier Debeir

Année académique 2013-2014

Contents

List of Figures

List of Tables

Chapter 1

Introduction

1.1 Introduction

The lymphatic system plays an important role in the human body. Not only it is responsible for fat absorption but also for fluid balance and immunological defense. The lymphatic system is part of the circulatory system, like the blood system. The blood is composed of blood cells and plasma, which contains proteins and carries the white cells. The plasma goes through the capillary vessels in order to reach all the human body cells therefore the entire cells bath in this filtered blood called lymph.

This lymph has to be cleaned and recirculated, which is why the lymphatic system is used for. It takes back the lymph, makes it circulate through the human body and then returns it to the blood. In addition, the lymphatic system is composed of lymph nodes, which filter the lymph and create lymphocytes to combat invaders and protect the body.

As opposed to the blood circulatory system, the lymphatic system does not have a pump to make the lymph circulate; it uses muscles and breathing motion to pump the lymph through the body.

The study of the lymphatic system is important for cancer diagnoses and treatments. Indeed, metastasis can circulate quickly in the lymphatic system and spread the tumor cells to other parts of the body. In addition, tissue swelling called lymphedema can occur after cancer surgery, it is especially the case after breast cancer surgeries [23]. In order to treat the lymphedema,

massage can be applied to drain the lymph fluid through the patient body and increase the lymph circulation.

The lymphatic system has a complex structure and varies greatly among individuals. Therefore, visualizing it correctly is a tremendous task, which requires the use of methods able to deliver accurate structural information. The lymphatic system structure can be seen in Figure 1.1 [6].

Figure 1.1.The lymphatic system

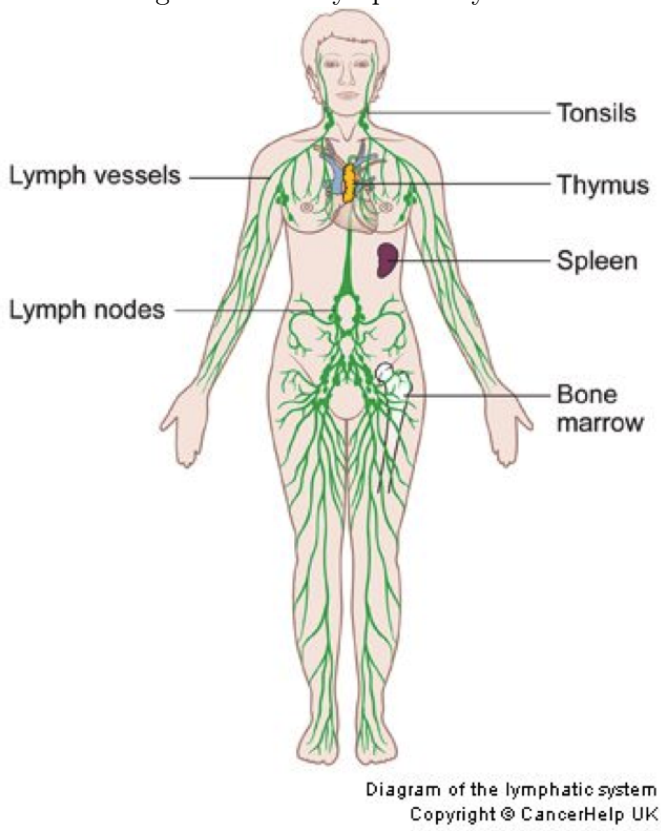

According to [23] "The lack of imaging to obtain structural or functional information currently limits our understanding of the role of lymphatics in disease and impedes the development of therapeutic interventions" therefore this paper introduces a novel imaging method for the lymphatic system, using infrared lights coupled with a 3D camera.

1.2 Purpose

The purpose of this project is to develop a 3D cartography tool to visualize the lymphatic system of an individual. In order to do that, a green dye called indocyanine green is injected into patients' lymphatic system. This dye has the property to be fluorescent after being exited by infrared lights therefore depth information can be acquired by using infrared cameras. However, the 3D structure only is not helpful because semantics has to be given to that 3D model, i.e. a mapping has to be applied between the lymphatic system's 3D model and the part of the human body corresponding to that 3D model (see Figure 1.2 and Figure 1.3 [4]).

Figure 1.2.Mapping of the lymphatic model with the corresponding body part

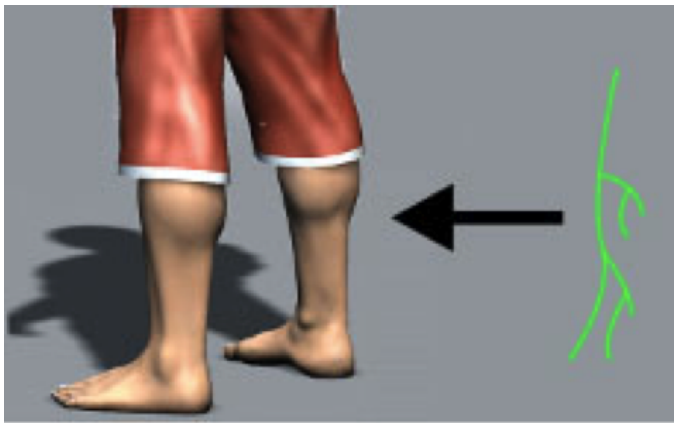

Figure 1.3.Mapping done

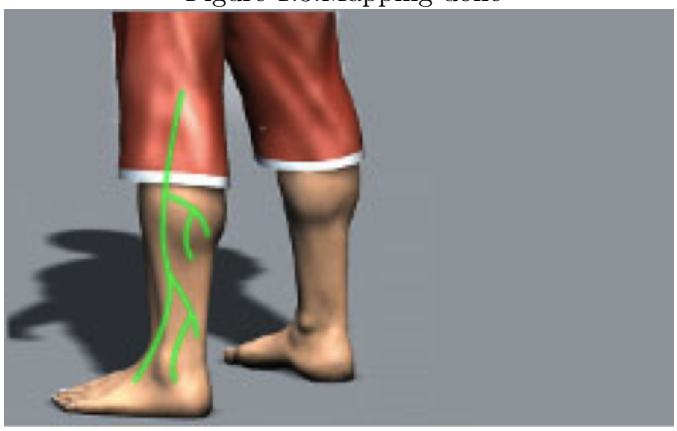

In order to do that, a 3D model of the human body is acquired through

a Microsoft Kinect camera. Given an accurate 3D model of a patient and his lymphatic system, the mapping can be easily done and physicists and physiotherapists can therefore operate more easily on the patients (see Application).

Furthermore, because the cameras do not have a wide field of vision, image fusion and camera pose estimation have to be used. Image fusion consists of combining multiple images into one while camera pose estimation consists of translating the camera coordinate system into a world coordinate system.

This master thesis will be about creating a prototype model for testing purposes (see Figure 1.4). This prototype model will be a basic representation of a human body limb. In the first time, a basic Kinect camera will be used to acquire a 3D representation of the prototype. If this step is successful, an infrared camera will be introduced with the use of indocyanine green.

Figure 1.4.Prototype model

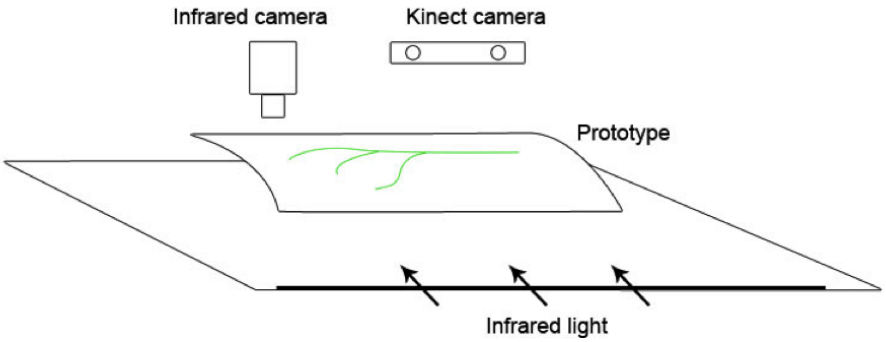

Chapter 2

State of the art

2.1 Introduction

This literature review uses a bottom-up approach in order to describe the whole system. To construct a 3D representation of the lymphatic system, different disciplines have to be combined. First, this paper describes the biochemical process of the near-infrared fluorescence principle, a brief explanation is given and the indocyanine green solution is introduced. In addition, this paper reviews in which applications the indocyanine green is used and in what purposes. Third, the different lymphatic system imaging techniques are reviewed. Furthermore, an introduction to the Kinect, its solution to 3D surface reconstruction and the camera pose estimation problem are presented. Finally, the OpenCV library is presented. Indeed, an infrared camera will be used in addition of the Kinect camera therefore its pose estimation has to be computed too. OpenCV provides many useful functions to solve the pose estimation problem. Moreover, OpenCV offers solutions to other problems such as camera calibration and image stitching.

2.2 Fluorescence principle

The fluorescence principle is a phenomenon in which molecules (called fluorochromes) emit light after being excited with light from another source. Fluorescence imaging offers many advantages over other imaging techniques such as ultrasound and x-ray fluoroscopy [30]. In addition, fluorochromes can be repeatedly exited even after returning to their ground state [23]. However, not all wavelengths of light are suitable. Bellow 700nm the depth of tissue penetration by light is too shallow, above 900nm water absorption in-

terferes with the signal-to-background ratio [18]. The region between 700nm and 900nm corresponds to the near-infrared region (NIR) therefore NIR fluorochromes are commonly used for fluorescence imaging. Since the NIR is invisible for human eyes and the emitted light is from a different wavelength of the projected light, the location of the fluorochromes have to be determined using a specific optical imaging device such an infrared camera.

The indocyanine green (ICG) is a commonly used NIR fluorochrome and it is the only one used in human studies [23]. ICG is an excellent vascular agent for the blood and lymphatic systems and it does not need to be used in large quantities. However, it has weak fluorescence properties but can be exited at a range between 760nm and 785nm with an emitted light between 820 and 840 nm.

Finally, ICG presents only a low toxicity [22] because it is not absorbed by the intestinal membrane but rejected via the liver.

2.3 ICG Applications

The ICG has been used in the medical field for more than 50 years. Cherrick et al. (1960) [11] used the ICG as an agent to estimate the hepatic blood flow on patients. However, it is only recently that ICG is used as a contrast agent when using NIR cameras. Murawa et al. (2009) [25] used ICG for lymphatic mapping and sentinel lymph node biopsy in breast cancer. Handa et al. (2009) [15] used it to capture near-infrared images during coronary artery bypass graft.

Miyashiro et al. (2008) [24] concluded that ICG is a promised tool to detect sentinel node in gastric cancer surgery. According to Marshall et al. (2012) [23] "To date, clinical applications range from (i) angiography, intraoperative assessment of vessel patency, and tumor/metastasis delineation following intravenous administration of ICG, and (ii) imaging lymphatic architecture and function following subcutaneous and intradermal ICG administration".

All these studies were conducted using ICG as a 2D imaging tool. In a recent study, Liu et al. (2011) [20] stated that "2-D imaging systems do not

provide sufficient depth information to guide an operation that is essentially three-dimensional". Therefore, this master thesis will investigate this problem using ICG and NIR cameras.

A 3D cartography of the lymphatic system can be used in 2 different applications:

- Locate and cut lymph node during surgery to prevent metastasis spread.
- Post-surgery application: treat lymphedema with massages.

2.4 Lymphatic system imaging techniques

The traditional imaging technique for the lymphatic system was the lymphography [14], which consists of injecting a radio contrast agent into a patient's body and then taking a X-Ray picture. Nowadays, common techniques are computed tomography (CT) and magnetic resonance imaging (MRI) [14, 28]. CT and MRI can be done with or without contrast agents [21]. In addition to these techniques, newer ones exists such as positron emission tomography, dynamic contrast-enhanced MRI (DCE-MRI) and color Doppler ultrasound (CDUS), which can provide more functional information than the CT and MRI scan [8].

It is only recently that fluorochromes such as ICG are used to obtain images of the lymphatic structure. According to Rasmussen et al. (2009) [27] "NIR fluorescence imaging has the opportunity to provide more rapid imaging of lymphatic function". However, they stated that "Although ICG has successfully been used to image the lymphatics, it possesses limitations such as a low quantum efficiency (0.016), which may limit the signal strength for deep interrogation of tissues and future tomography applications [33–36]" therefore in the future new dyes have to be developed and tested on humans. The following table shows the review study conducted by Rasmussen et al. [27]

Table 2.1: Review of fluorescence imaging of the lymphatics.

Author, Year [ref]	# of Subjects	Study Aim	Dosage	Comments
Kitai et al., 2005,[28]	18	Sentinel lymph node mapping and resection in breast cancer patients.	Unspecified amount of 5mg/ml ICG	Observed subcutaneous lymphatic vessels in all patients and identified sentinel nodes in 17 patients. No active propulsion reported.
Ogata et al., 2007, [31]	5	Intraoperative guidance for persons with lymphedema.	1 mg ICG	Used fluorescence imaging to intraoperatively guide lymphaticovenular anastomoses for treatment of lymphedema.
Unno et al., 2007, [25]	22	Diagnose lymphedema using fluorescence imaging.	1 mg ICG	Imaged and compared the lymphatics of 10 normal subjects and 12 subjects with secondary lymphedema of the leg. Identified characteristic fluorescent features in lymphedema subjects and compared to lymphoscintigraphy.

Fujiwara et al., 2008, [29]	10	Sentinel lymph node mapping and resection in skin cancer patients.	Unspecified number of injections containing 0.5 mg ICG	Successfully observed and identified lymphatic vessels and sentinel nodes in all subjects. No active propulsion was reported.
Sevick-Muraca et al.,2008, [26]	24	Dose escalation study for sentinel lymph node mapping in breast cancer patients.	0.31–100 μg ICG	Established minimal dosage of ICG needed to observe lymphatic trafficking to sentinel nodes. To our knowledge is the first time active lymphatic propulsion was observed in humans.
Ogasawara et al., 2008,[27]	37	Evaluate breast lymphatic pathways in patients with breast cancer.	25 mg ICG	Monitored lymph drainage pathways from different areas of the breast to the axilla.

Unno et al., 2008, [24]	27	Measure transit times of dye from injection to knees and inguinal region.	1.5 mg ICG	Imaged and compared transit times to knee and groin of 10 normal subjects and 17 subjects undergoing abdominal aortic aneurysm treatment. Correlated fluorescent velocities with lymphoscintigraphy velocities. Reported pulsatile flow in one lymphatic vessel.
Sevick-Muraca and Rasmussen, 2008, [32] Sharma et al., 2008, [6]	44	An ongoing study to quantitatively compare lymph function between normal and lymphedema subjects.	100–400 μg ICG	These papers provided snapshots of an ongoing clinical trial of lymphatic function. Velocity and period of propulsive flow were calculated, and the structure of normal and diseased lymphatics investigated.

2.5 3D surface reconstruction

A 3D camera Kinect will be used to construct a 3D representation or the patient's limb. A Kinect camera is constituted of a RGB camera, a depth sensor and an infrared light emitter (see Figure 2.1 [1]).

Figure 2.1.The Kinect camera

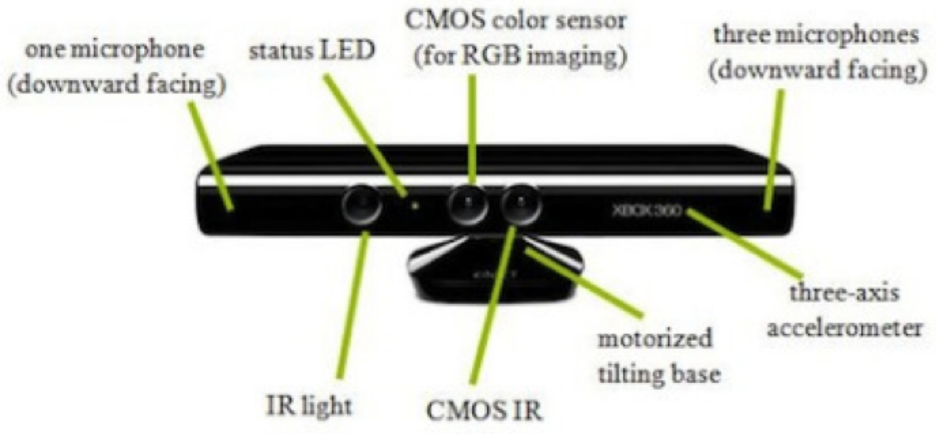

Because of its depth camera and infrared light emitor, the Kinect is able to provide a live depth map using a technique called structured light [13], which consists of projecting a known pattern of infrared dots into the scene and determine the depth by analyzing the pattern deformation. The kinect hardcodes all the information about the pattern (the dots and their relative distances) thus it can compare what it sees with what it stores and provide a live depth map of the scene (see Figure 2.2 [19]).

Figure 2.2.A depth map from the Kinect camera

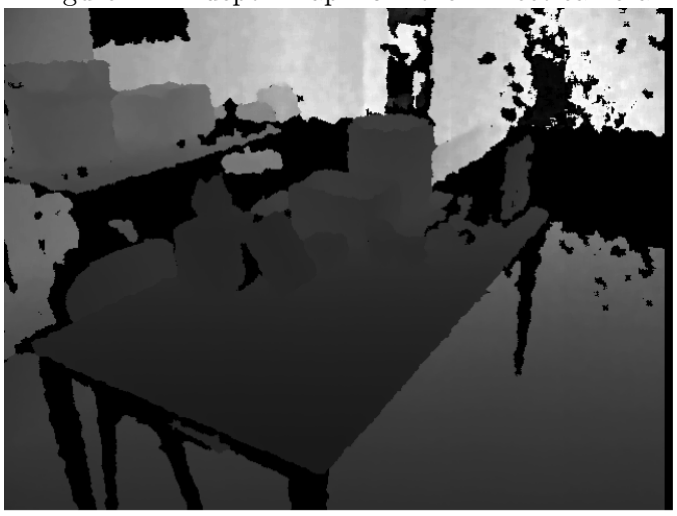

The Microsoft Kinect has the advantage to be relatively low cost and offers many useful API included the KinectFusion toolkit. KinectFusion provides fast 3D surface reconstruction by scanning the object with the Kinect

camera only. In addition, KinectFusion is fast and takes care of low level problems such as camera calibration (see section 2.6), camera pose, surface reconstruction...

The researches about KinectFusion started in 2011 by Shahram Izadi et al. [16]. Explaining in details the implementation of KinectFusion is beyond the scope of this state of art and more details can be found in [26] and [16]. However, an interesting problem is the camera pose problem. The camera pose problem consists of transforming the camera coordinate system into a global coordinate system. In order to solve the camera six degrees of freedom (6DOF) pose, KinectFusion uses the iterative closest point (ICP) algorithm.

The ICP algorithm is an algorithm used to find the transformation that minimizes the distance between two set of points. ICP is normally used to reconstruct 3D surfaces from different views of the same object. However, KinectFusion uses it to obtain a 6DOF transform that aligns the current points with the ones from the previous depth frame. This transform therefore gives the Kinect global camera pose.

One of the key features of the KinectFusion algorithm is its parallel execution [16] on the GPU thus fast camera tracking and real-time 3D reconstruction can be obtained. In consequence of that, only compatible DirectX11 graphics cards can meet the requirement to run KinectFusion [5].

Using 3D surface reconstruction tools like the KinectFusion solves the problem of acquiring a 3D surface of the prototype to map the lymphatic system on it. In addition, image fusion, camera calibration and 6DOF pose solution are offered by the KinectFusion toolkit. However, the Kinect camera cannot be used only to obtain information about the lymphatic system. Indeed, fluorochromes will emit infrared lights as well and even though those infrared lights will be in a different range of the ones emitted from the Kinect camera, they can perturb the collected data. Therefore, a separated infrared camera will be used.

2.6 3D cartography method

The 3D cartography of the lymphatic system will be the most complex step of this master thesis. It will require solving the camera pose (see 3D surface reconstruction), camera calibration and image stitching problems. Fortunately, all these problems can be solved more easily by using the OpenCV (Open Source Computer Vision) library.

OpenCV is a free library used in computer vision and real-time applications. It is written in C++ and has C, python and java interfaces. In addition, OpenCV is cross-platform and provides more than 2500 optimized algorithms [7] which can be used for camera tracking, face recognition, image stitching, augmented reality, etc.

The following paragraphs will cover briefly how OpenCV can be used to solve the previous mentioned problems. A deeper explanation will be given afterwards when the project will start.

2.6.1 Camera calibration

Before explaining what a camera calibration is and how OpenCV does it, some explanations about basic camera functioning must be given. The figures and formulas in the following paragraphs come from the work of Bradski et al. (2008) [10], the reader is invited to consult their book for further information.

First of all, the simplest camera model is the pinhole camera, in which the light going through a small hole is projected in the opposite surface of that hole. See Figure 2.3 [10, p. 372]. X is the length of the object, x is the projected object image, Z is the distance from the camera to the object and f is the focal length, i.e. the distance where converging/diverging rays are in a focus point.

Like with the human eye, the projected image is inverted, which gives the following equation taken from [10, p. 371] (see the relation between the

Figure 2.3.The Pinhole camera model

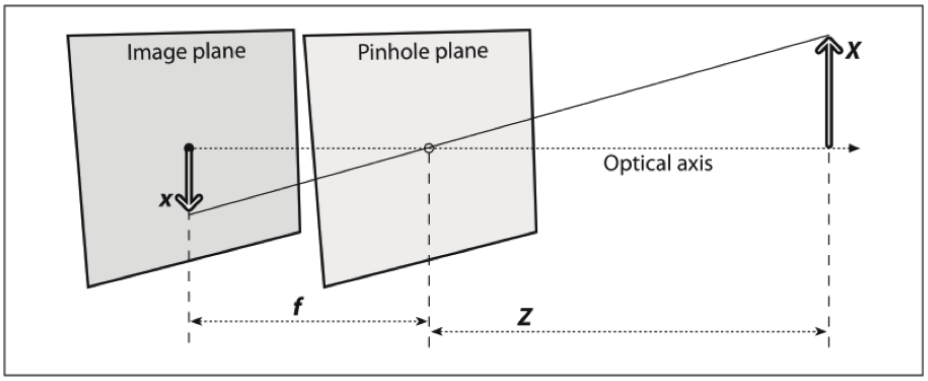

two triangles):

$$-x = f\frac{X}{Z} \tag{2.1}$$

Now, in order to eliminate the negative sign, the following model [10, p. 372] can be used instead of the one showed in Figure 2.3 (notice that the relation between the two triangles is still valid):

Figure 2.4.Simplified pinhole camera model

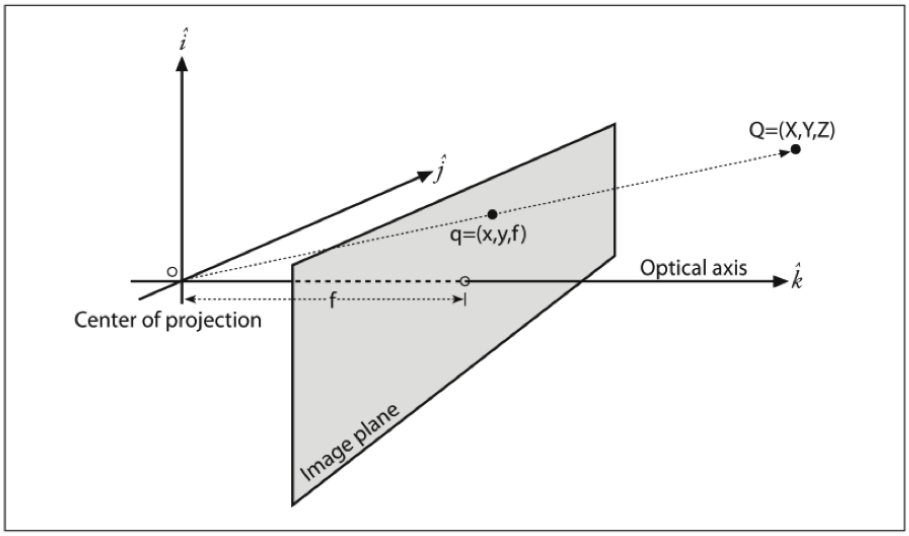

Next, two parameters c_x and c_y must be introduced. Indeed, one might think that the intersection of the projection center (see Figure 2.4) with the image plane is exactly at the center of the image plane. However, it is

often not the case therefore these two parameters are used to adjust this displacement. The following formulas [10, p. 373] give the coordinates of a point in the image plane.

$$x = f_x \left(\frac{X}{Z}\right) + c_x \quad y = f_y \left(\frac{Y}{Z}\right) + c_y \tag{2.2}$$

Finally, the following matrices [10, p. 374] give the transformation that maps a point in the physical world with a point in the image plane. Q is a one-column matrix representing a point in the physical world while q represents the image plane point; q is a 3 dimensions vector because homogeneous coordinates are used. M is called the camera intrinsic matrix.

$$q = MQ \tag{2.3}$$

$$q = \begin{bmatrix} x \\ y \\ w \end{bmatrix}, M = \begin{bmatrix} f_x & 0 & c_x \\ 0 & f_y & c_y \\ 0 & 0 & 1 \end{bmatrix}, Q = \begin{bmatrix} X \\ Y \\ Z \end{bmatrix} \tag{2.4}$$

The pinhole camera model is simple but unfortunately the real cameras use lenses in order to gather more light. Lenses introduce some distortions, which have to be corrected. Two different distortions exist, radial distortions and tangential distortions [10, p. 375].

Radial distortions can be corrected by the following formulas:

$$x_{corrected} = x(1 + k_1 r^2 + k_2 r^4 + k_3 r^6) \tag{2.5}$$

$$y_{corrected} = y(1 + k_1 r^2 + k_2 r^4 + k_3 r^6) \tag{2.6}$$

Tangential distortions can be corrected by the following formulas:

$$x_{corrected} = x + [2p_1 y + p_2(r^2 + 2x^2)] \tag{2.7}$$

$$y_{corrected} = y + [p_1(r^2 + 2y^2) + 2p_2 x] \tag{2.8}$$

Therefore, in addition with the intrinsic matrix, a 5-by-1 matrix containing the k_1, k_2, p_1, p_2 and k_3 parameters has to be solved. Determining these two matrices is exactly what the calibration process is used for.

OpenCV uses the cvCalibrateCamera2() function to do the calibration. The user has to target the camera to a known pattern/structure, usually a chessboard [31]. By taking multiple snapshots of the chessboard at different angles, OpenCV can determine the intrinsic parameters [3].

In conclusion the camera calibration is used to correct distortions and obtain the transform matrix to determine the relation between the object coordinates and the image coordinates.

2.6.2 Camera pose estimation

As seen in the previous part, the equations 2.3 and 2.4 provide a way to map world coordinates into camera coordinates. However, those equations consider only the intrinsic camera parameters (the matrix M) and not the extrinsic parameters. A real camera is moving while recording multiple view of an object therefore the camera coordinates are different from the object/world coordinates for each frame. In consequence, for each frame, a transformation that transforms the object coordinate system into the internal camera coordinate system has to be found. This transformation is a combination of a rotation and a translation matrix.

The equations become [2]:

$$q = M\langle R|T\rangle Q \tag{2.9}$$

$$q = \begin{bmatrix} x \\ y \\ w \end{bmatrix}, M = \begin{bmatrix} f_x & 0 & c_x \\ 0 & f_y & c_y \\ 0 & 0 & 1 \end{bmatrix}, \langle R|T\rangle = \begin{bmatrix} r_{11} & r_{12} & r_{13} & t_1 \\ r_{21} & r_{22} & r_{23} & t_2 \\ r_{31} & r_{32} & r_{33} & t_3 \end{bmatrix}, Q = \begin{bmatrix} X \\ Y \\ Z \end{bmatrix} \tag{2.10}$$

The matrix M has to be computed only once but the transformation matrix $\langle R|T\rangle$ has to be computed every frame. In that purpose some markers will be placed in the camera field. Those markers will be easily identifiable by the camera (usually a known pattern is used like the chessboard) therefore their position q will be known. In addition, they will never change of position therefore the position Q will also be known thus determining the camera pose will only consist of solving the equation.

2.6.3 Image stitching

As mentioned before, because the camera does not have a wide field of vision, multiple overlapping images will have to be combined together to form only one. This process called image stitching can also be done with OpenCV.

In the first time OpenCV uses SURF descriptors [9] to find correspondences between two images targeting the same scene. Once the matching has been found, OpenCV finds the homography matrix to match the two images together.

2.7 Conclusion

The lymphatic system plays an important role for the body. Obtaining structural information about it is an important task in the medical field. This state of art gave a brief overview of the different problems that will occur during this project. The remaining part of this master thesis will consist of constructing a working prototype for testing purposes, obtaining a 3D construction of it through a Kinect camera and finally, obtaining 3D information from NIR fluorochromes. In that purpose, the OpenCV library and algorithms will be examined in more details.

Bibliography

[1] Build a kinect bot for 500 bones.

[2] Camera calibration and 3D reconstruction — OpenCV 2.0 c reference.

[3] Camera calibration with OpenCV — OpenCV 2.4.6.0 documentation.

[4] Gianluca MIragoli makehuman 3d characters | makehuman.

[5] Kinect fusion.

[6] The lymphatic system : Cancer research UK : CancerHelp UK.

[7] OpenCV | OpenCV.

[8] Tristan Barrett, Peter L. Choyke, and Hisataka Kobayashi. Imaging of the lymphatic system: new horizons. *Contrast Media & Molecular Imaging*, 1(6):230–245, 2006.

[9] Herbert Bay, Tinne Tuytelaars, and Luc Van Gool. Surf: Speeded up robust features. In *Computer Vision–ECCV 2006*, page 404–417. Springer, 2006.

[10] Gary R Bradski and Adrian Kaehler. *Learning OpenCV: computer vision with the OpenCV library*. O'Reilly, Sebastopol, CA, 2008.

[11] Gilbert R. Cherrick, Samuel W. Stein, Carroll M. Leevy, and Charles S. Davidson. Indocyanine green: observations on its physical properties, plasma decay, and hepatic extraction. *Journal of Clinical Investigation*, 39(4):592, 1960.

[12] Brian Curless and Marc Levoy. A volumetric method for building complex models from range images. In *Proceedings of the 23rd annual conference on Computer graphics and interactive techniques*, page 303–312, 1996.

[13] Barak Freedman, Alexander Shpunt, Meir Machline, and Yoel Arieli. Depth mapping using projected patterns, April 2008.

[14] Ali Guermazi, Pauline Brice, Christophe Hennequin, and Emile Sarfati. Lymphography: An old technique retains its usefulness1. *Radiographics*, 23(6):1541–1558, January 2003. PMID: 14615563.

[15] Takemi Handa, Rajesh G. Katare, Shiro Sasaguri, and Takayuki Sato. Preliminary experience for the evaluation of the intraoperative graft patency with real color charge-coupled device camera system: an advanced device for simultaneous capturing of color and near-infrared images during coronary artery bypass graft. *Interactive CardioVascular and Thoracic Surgery*, 9(2):150–154, January 2009. PMID: 19423513.

[16] Shahram Izadi, David Kim, Otmar Hilliges, David Molyneaux, Richard Newcombe, Pushmeet Kohli, Jamie Shotton, Steve Hodges, Dustin Freeman, and Andrew Davison. KinectFusion: real-time 3D reconstruction and interaction using a moving depth camera. In *Proceedings of the 24th annual ACM symposium on User interface software and technology*, page 559–568, 2011.

[17] Toshiyuki Kitai, Takuya Inomoto, Mitsuharu Miwa, and Takahiro Shikayama. Fluorescence navigation with indocyanine green for detecting sentinel lymph nodes in breast cancer. *Breast cancer (Tokyo, Japan)*, 12(3):211–215, 2005. PMID: 16110291.

[18] Joy L. Kovar, Melanie A. Simpson, Amy Schutz-Geschwender, and D. Michael Olive. A systematic approach to the development of fluorescent contrast agents for optical imaging of mouse cancer models. *Biochemistry–Faculty Publications*, page 9, 2007.

[19] Antoine Lejeune, Sébastien Pierard, Marc Van Droogenbroeck, and Jacques Verly. A new jump edge detection method for 3D cameras. In *International Conference on 3D Imaging (IC3D)*, 2011.

[20] Yang Liu, Adam Q. Bauer, Walter J. Akers, Gail Sudlow, Kexian Liang, Duanwen Shen, Mikhail Y. Berezin, Joseph P. Culver, and Samuel Achilefu. Hands-free, wireless goggles for near-infrared fluorescence and real-time image-guided surgery. *Surgery*, 149(5):689–698, May 2011.

[21] Alain Luciani, Emmanuel Itti, Alain Rahmouni, Michel Meignan, and Olivier Clement. Lymph node imaging: Basic principles. *European Journal of Radiology*, 58(3):338–344, June 2006.

[22] Hope-Ross M, Yannuzzi La, Gragoudas Es, Guyer Dr, Slakter Js, Sorenson Ja, Krupsky S, Orlock Da, and Puliafito Ca. Adverse reactions due to indocyanine green. *Ophthalmology*, 101(3):529–533, March 1994. PMID: 8127574.

[23] Milton V. Marshall, John C. Rasmussen, I.-Chih Tan, Melissa B. Aldrich, Kristen E. Adams, Xuejuan Wang, Caroline E. Fife, Erik A. Maus, Latisha A. Smith, and Eva M. Sevick-Muraca. Near-infrared fluorescence imaging in humans with indocyanine green: a review and update. *Open surgical oncology journal (Online)*, 2(2):12, 2010.

[24] Isao Miyashiro, Norikatsu Miyoshi, Masahiro Hiratsuka, Kentaro Kishi, Terumasa Yamada, Masayuki Ohue, Hiroaki Ohigashi, Masahiko Yano, Osamu Ishikawa, and Shingi Imaoka. Detection of sentinel node in gastric cancer surgery by indocyanine green fluorescence imaging: Comparison with infrared imaging. *Annals of Surgical Oncology*, 15(6):1640–1643, April 2008.

[25] D Murawa, C Hirche, S Dresel, and M Hünerbein. Sentinel lymph node biopsy in breast cancer guided by indocyanine green fluorescence. *The British journal of surgery*, 96(11):1289–1294, November 2009. PMID: 19847873.

[26] Richard A. Newcombe, Andrew J. Davison, Shahram Izadi, Pushmeet Kohli, Otmar Hilliges, Jamie Shotton, David Molyneaux, Steve Hodges, David Kim, and Andrew Fitzgibbon. KinectFusion: real-time dense surface mapping and tracking. In *Mixed and augmented reality (ISMAR), 2011 10th IEEE international symposium on*, page 127–136, 2011.

[27] John C. Rasmussen, I-Chih Tan, Milton V. Marshall, Caroline E. Fife, and Eva M. Sevick-Muraca. Lymphatic imaging in humans with near-infrared fluorescence. *Current opinion in biotechnology*, 20(1):74–82, February 2009. PMID: 19233639 PMCID: PMC2692490.

[28] Michael J. Reinhardt, Claudia Ehritt-Braun, Dagmar Vogelgesang, Christian Ihling, Stefan Högerle, Michael Mix, Ernst Moser, and

Thomas M. Krause. Metastatic lymph nodes in patients with cervical cancer: Detection with MR imaging and FDG PET1. *Radiology*, 218(3):776–782, January 2001. PMID: 11230656.

[29] Eva M. Sevick-Muraca, Ruchi Sharma, John C. Rasmussen, Milton V. Marshall, Juliet A. Wendt, Hoang Q. Pham, Elizabeth Bonefas, Jessica P. Houston, Lakshmi Sampath, Kristen E. Adams, Darlene Kay Blanchard, Ronald E. Fisher, Stephen B. Chiang, Richard Elledge, and Michel E. Mawad. Imaging of lymph flow in breast cancer patients after microdose administration of a near-infrared fluorophore: Feasibility study1. *Radiology*, 246(3):734–741, January 2008. PMID: 18223125.

[30] Susan L. Troyan, Vida Kianzad, Summer L. Gibbs-Strauss, Sylvain Gioux, Aya Matsui, Rafiou Oketokoun, Long Ngo, Ali Khamene, Fred Azar, and John V. Frangioni. The FLARE$^{\text{TM}}$ intraoperative near-infrared fluorescence imaging system: A first-in-human clinical trial in breast cancer sentinel lymph node mapping. *Annals of Surgical Oncology*, 16(10):2943–2952, July 2009.

[31] Zhengyou Zhang. Flexible camera calibration by viewing a plane from unknown orientations. In *Computer Vision, 1999. The Proceedings of the Seventh IEEE International Conference on*, volume 1, page 666–673, 1999.